NANO · MICRO small
www.small-journal.com

Graphene Oxide "Surfactant"-Directed Tunable Concentration of Graphene Dispersion

Jiajun Luo, Liangwei Yang, Danping Sun, Zhenfei Gao, Kun Jiao, and Jin Zhang**

Homogeneous graphene dispersions with tunable concentrations are fundamental prerequisites for the preparation of graphene-based materials. Here, a strategy for effectively dispersing graphene using graphene oxide (GO) to produce homogeneous, tunable, and ultrahigh concentration graphene dispersions (>150 mg mL^{-1}) is proposed. The structure of GO with abundant edge-bound hydrophilic carboxyl groups and in-plane hydrophobic π-conjugated domains allows it to function as a special "surfactant" that enables graphene dispersion. In acidic solutions, GO sheets tend to form edge-to-edge hydrogen bonds and expose the π-conjugated regions which interact with graphene, thereby promoting graphene dispersion. While in alkaline solutions, GO sheets tend to stack in a surface-to-surface manner, thereby blocking the π-conjugated regions and impeding graphene dispersion. As the concentration of GO-dispersed graphene dispersion (GO/G) increases, a continuous transition between four states is obtained, including a dilute dispersion, a thick paste, a free-standing gel, and a kneadable, playdough-like material. Furthermore, GO/G can be applied to create desirable structures including highly conductive graphene films with excellent flexibility, thereby demonstrating an immense potential in flexible composite materials.

1. Introduction

As the thinnest carbon material, graphene possesses unique and extraordinary mechanical, electrical, and thermal properties by virtue of its honeycomb-lattice arrangement of atoms.[1,2] Although graphene has been used in many fields,[3–7] its remarkable properties are only observed on a molecular level and cannot be effectively utilized in macroscopic graphene-based materials. Thus, to more widely apply graphene intrinsic superior properties in various fields, it is necessary and extremely important to build a bridge to transfer the excellent microscopic properties of graphene to macroscopic graphene-based materials.[8] In this regard, the preparation of homogeneous, stable graphene dispersions is one of the key issues. However, the main challenge for dispersing graphene nanosheets in aqueous solution is their tendency to agglomerate because of the mismatch of surface tensions and strong π–π interactions between the large sp^2-conjugated structures.[9,10] To date, two feasible strategies have been generally adopted to address this problem. The first involves the noncovalent functionalization of graphene using specific polymers, surfactants, or conjugated aromatic small molecules as stabilizers (such as polyvinylpyrrolidone, diazaperopyrenium dications, or pyrenes).[11–19] The second strategy employs the covalent functionalization of graphene, increasing its hydrophilicity by grafting functional moieties such as hydroxyl, carboxyl, or amino groups.[20–23] However, covalent functionalization can destroy the original perfect structure and affect the microscopic properties of graphene; meanwhile, noncovalent functionalization usually introduces impurities into the system which may affect the transfer of microscopic properties to macroscopic properties.[10] Therefore, developing an efficient dispersion method that can maximally maintain and transfer the microscopic properties of graphene remains an urgent and challenging problem.

Besides, obtaining tunable and ultrahigh concentration graphene dispersions is critical to the applications of graphene in different fields. For example, low-concentration graphene dispersions can be used to make the conductive film and heat dissipation film;[24–26] high-concentration graphene dispersions can be spun into high-performance graphene fibers[27,28] and ultrahigh concentration graphene dispersions can be used for energy storage.[29] So far, low-concentration graphene dispersions are easily obtained using traditional graphene dispersants. However, it is difficult to prepare high-concentration or ultrahigh concentration graphene dispersions due to the requirement of a high concentration of dispersant, which inevitably can cause

J. Luo, Dr. L. Yang, Dr. D. Sun, Dr. Z. Gao, Dr. K. Jiao, Prof. J. Zhang
Center for Nanochemistry
Beijing Science and Engineering Center for Nanocarbons
Beijing National Laboratory for Molecular Sciences
College of Chemistry and Molecular Engineering
Peking University
Beijing 100871, P. R. China
E-mail: jinzhang@pku.edu.cn

J. Luo, Prof. J. Zhang
Academy for Advanced Interdisciplinary Studies
Peking University
Beijing 100871, P. R. China

J. Luo, Dr. L. Yang, Dr. D. Sun, Dr. Z. Gao, Dr. K. Jiao, Prof. J. Zhang
Beijing Graphene Institute (BGI)
Beijing 100095, P. R. China
E-mail: jiaokun@bgi-graphene.com

Dr. L. Yang
Research Institute of Aerospace Special Materials
and Processing Technology
Beijing 100074, P. R. China

The ORCID identification number(s) for the author(s) of this article can be found under https://doi.org/10.1002/smll.202003426.

DOI: 10.1002/smll.202003426

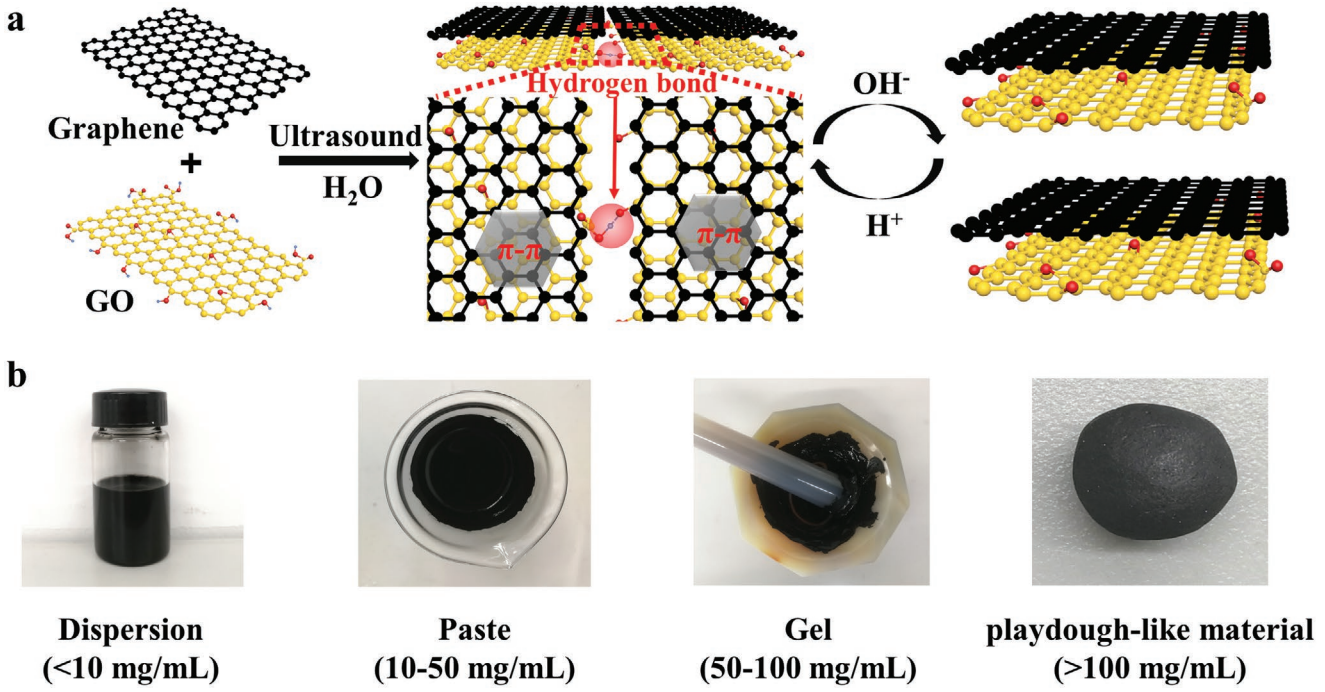

Figure 1. a) Schematic illustration of graphene dispersion using GO as a special "surfactant." The addtion of OH^- will destroy the edge-to-edge hydrogen bonds between GO sheets and form stable graphene dispersion. b) Four continuous physical states as a function of GO/G concentration, including a dilute dispersion, a thick paste, a free-standing gel, and a kneadable, playdough-like material.

the instability of graphene dispersions. First, the solubility of some dispersants is relatively small, which cannot meet the requirements. Second, it is difficult to combine the dispersant and graphene homogeneously at high concentration. Therefore, exploring a suitable graphene dispersant remains a top priority.

The noncovalent functionalization of graphene should be the most suitable option for maximally retaining its intrinsic properties. Surfactants are 1D chain-like molecules consisting of hydrophilic heads and hydrophobic tails that can adsorb at interface and reduce the surface tension of the solvent.[30] Several small organic molecules possessing aromatic planar surfaces and functional polar or apolar groups decorating the aromatic core have been used as surfactants to disperse graphene.[9,12,13,15,31] Compared with these small organic molecules, graphene oxide (GO) contains a mass of larger hydrophobic π-conjugated regions as well as epoxy groups and hydroxyl groups on the basal plane, and more hydrophilic carboxyl groups at the edges.[32–35] Because of its special amphiphilic properties, GO can be stably dispersed in aqueous solutions at ultrahigh concentration and adhere to and activate the interface. For example, GO in aqueous solution can exhibit from low-concentration dispersions to high-concentration dense solids with the increase of GO concentration.[29] What is more, GO can be captured by the rising bubble of aqueous solution and then transported to the water surface to activate the interface.[36,37] Therefore, GO could be expected to act as a special "surfactant" to disperse graphene through π–π interactions between the π-conjugated basal plane in aqueous solution with high concentration.[38,39] Owing to the structural similarity between GO and graphene, the prepared macroscopic graphene-based materials may maximally maintain intrinsic properties of graphene.

Herein, we report an efficient "surfactant"-GO that effectively disperses graphene through π–π interactions in acidic aqueous solutions, without the need for any additives. In acidic solutions, GO sheets tend to form edge-to-edge hydrogen bonds and expose the π-conjugated regions, which interact with graphene, thereby promoting dispersibility. In contrast, GO sheets tend to stack in a surface-to-surface manner in alkaline solutions, thereby blocking the π-conjugated regions and impeding graphene dispersion. Stable, homogeneous graphene dispersions at unprecedentedly high concentrations (>150 mg mL^{-1}) can be obtained by adjusting the pH value to make the dispersion alkaline, as shown in **Figure 1**a. In addition, as the concentration of GO-directed graphene dispersion (GO/G) increases, a continuous transition between four states is observed, including a dilute dispersion, a thick paste, a free-standing gel, and, eventually, a kneadable, playdough-like material (Figure 1b). These four states can be further transformed into 1D graphene fibers, 2D graphene films, and 3D graphene doughs through a broad array of material-processing techniques.

2. Results and Discussion

2.1. The Structure and Interface Activity of GO

In order to determine the ability of GO to disperse graphene, the structure of GO was considered first. GO was analyzed by X-ray photoelectron spectroscopy (XPS) to evaluate the chemical states of various elements and the presence of functional groups. The survey scan spectra of all samples (Figure S1, Supporting Information) show the presence of carbon and oxygen

with a trace amount of sulfur, which was a result of process contamination. High-resolution XPS spectra of C 1s region and O 1s region give detailed information (Figure S2, Supporting Information). The deconvoluted C 1s peaks 1, 2, 3, 4, and 5 show peak binding energies of 291.82, 289.44, 287.91, 286.52, and 284.60 eV, which correspond to π–π^* satellite bonds, O—C=O, C=O, C—O, and C—C, respectively. The deconvoluted O 1s peaks 1, 2, 3, and 4 with binding energies of 533.92, 532.98, 532.55, and 531.38 eV represent the C—O—C, C—OH, C=O, and O—C=O groups, respectively.[40–43] These fully show that GO has rich functional groups, such as carboxyl, hydroxyl, and epoxy groups, which make GO have better water solubility and can be stably dispersed in aqueous solution. In a typical GO structure, the carboxyl groups are mainly distributed at the edge, hydroxyl and epoxy groups are mainly on the basal plane, and there are also a large number of holes and hydrophobic π-conjugated regions.[44]

Based on its special amphiphilic properties, GO exhibits interfacial activity and can form Pickering emulsions at the water–oil interface, similar to surfactants.[37] To probe these phenomena in detail, we mixed GO aqueous solutions at different pH values with organic solvents and studied their emulsification properties. As pH value increases, the volume of the Pickering emulsion formed between GO aqueous solution and *n*-hexane decreases, and the Pickering emulsion droplets become larger (Figure S3, Supporting Information), meaning that the ability of GO to form Pickering emulsion gradually decreases, and the interfacial activity becomes weaker. This is due to the deprotonation reaction of edge-bound carboxyl groups of GO to produce more hydrophilic carboxylate ions, which leads to the enhanced hydrophilic properties of GO, thereby reducing its interfacial activity. More importantly, when *n*-hexane is replaced by π-conjugated toluene, the volume of Pickering emulsion becomes larger, and the droplets become smaller (Figure S4a, Supporting Information). Moreover, with the increase of GO concentration, the tendency to form a Pickering emulsion with toluene is more pronounced than that with *n*-hexane (Figures S4b, S5, and S6, Supporting Information). Results above indicate that GO can interact with toluene through its π-conjugated basal plane regions to form more stable Pickering emulsion. These results further illustrate that the amphiphilic properties of GO depend not only on its edge-bound carboxyl groups but also on its π-conjugated basal plane regions.

An efficient dispersant for dispersing graphene usually exhibits two basic characteristic: a high affinity toward graphene and good compatibility with the dispersing medium.[4] GO that contains a large number of π-conjugated regions on its basal plane has the potential to interact with graphene via π–π interactions to achieve the dispersion of graphene.[39,45,46] Besides, owing to the presence of numerous hydrophilic carboxyl groups at the edges of GO, it can be stably dispersed in aqueous solution. These factors inspired us to use GO as a special "surfactant" to disperse graphene in aqueous solution by changing its interfacial activity.

2.2. Performance of GO as a Graphene Dispersant

To verify the capability of GO as a special dispersant for graphene in water, graphene powder was characterized in detail. Low-resolution transmission electron microscopy (TEM) and atomic force microscopy (AFM) indicate that the average size of graphene is about 3.2 µm (**Figure 2**a; Figure S7, Supporting Information). High-resolution TEM shows that graphene that we used was with few layers, consistent with the results of AFM (Figure 2b).

To achieve the dispersion of graphene, commercial and high-concentration GO dispersion was first diluted with deionized water to homogeneous and low-concentration GO dispersion with an average size of ≈620 nm and a pH value of ≈5–6 by an ultrasonic process (Figure S8, Supporting Information). Then,

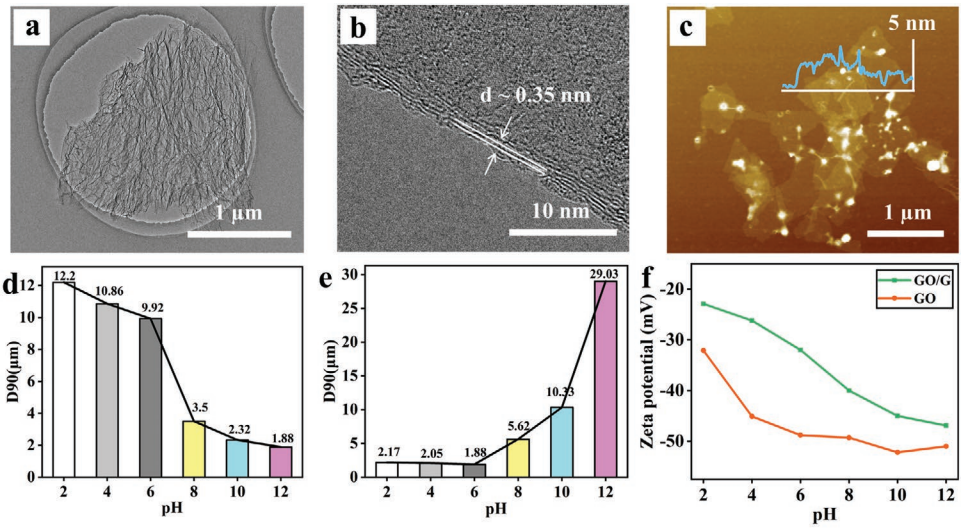

Figure 2. a) Low-magnification TEM image of graphene. b) High-resolution TEM image of the edge of graphene and a layer spacing of ≈0.35 nm can be observed. c) AFM image of GO/G; the inset shows the thickness of GO/G hybrid. d) Effect of the pH of GO/G on the GO/G sheets size (pH value of GO aqueous solution is 6, m_{GO}:m_G = 1:2). e) Effect of pH of GO aqueous solution on GO/G sheets size (pH value of GO/G is 12, m_{GO}:m_G = 1:2). f) Zeta potential of GO aqueous solution and GO/G as a function of pH (c_{GO} = 0.05 mg mL^{-1}, m_{GO}:m_G = 1:2).

graphene powder with an appropriate proportion was added to above GO dispersion and was sonicated with suitable power for a certain time (Figure S9, Supporting Information). As expected, a stable and homogeneous graphene dispersion was obtained in the aqueous solution. Further, compared with graphene dispersed in water, no distinct sedimentation of GO/G is observed (Figure S10, Supporting Information).

However, after shaking GO/G, floccules and sediments visible to the naked eye appear quickly. Interestingly, when the pH value of the solution is adjusted above 8 using NaOH solution (pH = 13), the floccules quickly disappear, a stable and homogeneous dispersion is achieved. Figure 2c displays a typical AFM image of GO/G hybrid. It should be noted that when the alkaline GO/G is adjusted to acidic with HCl solution (pH = 1), the floccules reappear (Figure S11, Supporting Information). The scanning electron microscope (SEM) images provide direct evidence for the dispersion states of GO/G with different pH values (Figure S12, Supporting Information). Under the acidic environment, GO/G sheets appear agglomeration, whereas, under the alkaline environment, a uniformly dispersed state is observed.

Optimizing the pH values of GO solution before adding graphene powder and GO/G can effectively improve the homogeneity and stability of GO/G. First, we examined the effect of the pH values of GO/G on dispersion stability (Figure 2d). A laser particle size analyzer was used to study sheets' size. The measurements obtained provide a means of monitoring dispersion stability.[47] As pH value increases, the size of GO/G sheets gradually decreases, which indicates the improving stability of GO/G. Besides, zeta potential was further used to study the stability of the dispersion (Figure 2e). With the increase of pH value, the absolute value of the zeta potential of the dispersion increases, which means that the dispersion is more stable. Especially, when the pH value is 12, the corresponding absolute value of the zeta potential is very high (46.9 mV), indicating that graphene dispersion is very stable and homogeneous. In addition, graphene dispersion can still exist stably after half a year of storage (Figure S13, Supporting Information). Based on the optimal pH value of GO/G, the effect of pH values of GO aqueous solution on dispersion stability was further investigated. Here, GO aqueous solutions with different pH values were used to disperse graphene in aqueous solution, respectively. Then, after the dispersion of graphene, the pH value was adjusted to 12. In Figure 2f, as the pH value of GO aqueous solution increases, the size of GO/G sheets grows larger; especially when it comes to alkaline environment, the sheet size shows a sharp increase, meaning the inability to disperse graphene. Thus, to prepare a homogeneous, stable GO/G, two conditions must be satisfied: the GO aqueous solution before adding graphene powder must be weakly acidic and the final graphene dispersion must be in an alkaline environment.

One of the criteria for evaluating the stability of graphene dispersion is the sedimentation rate. As the pH value of GO/G increases, the sedimentation rate decreases. Especially, at pH = 12, the sedimentation rate of GO/G is only 5.5%, indicating that GO/G has extremely high stability in alkaline environment (Figure S14, Supporting Information). In addition, dispersion capability of GO as a special "surfactant" for graphene was also investigated. As the graphene content increases, the size of GO/G sheets steadily grows (Figure S15a, Supporting Information). Besides, when m_{GO}:m_G > 1:2, two peaks appear (Figure S15b, Supporting Information), which implies that part of the graphene cannot be dispersed and suggests that the capability of GO to disperse graphene is twice the wight of GO itself. To further verify the dispersion capability, graphene films were prepared by filtering the dilute dispersion with different weight ratios (Figure S16, Supporting Information). As the graphene content increases, the square resistance of the corresponding graphene film decreases. Especially, when m_{GO}:m_G = 1:2, the square resistance of the graphene film exhibits a sharp drop. GO itself has essentially poor electrical conductivity.[24] The conductivity of graphene film comes from the construction of graphene network. When m_{GO}:m_G > 1:2, the low graphene content is insufficient for graphene sheets to make contact with each other on the surface of GO, leading to the poor conductivity of graphene film. However, when m_{GO}:m_G ≤ 1:2, graphene sheets are capable of interacting with each other and build a conductive path, resulting in a highly conductive graphene film (Figure S17, Supporting Information).

In order to verify the universality of GO as a special "surfactant" to disperse graphene, small-sized graphene (S-G) was also used for dispersion. Low-resolution TEM and AFM indicate that the average size of graphene is about 310 nm. High-resolution TEM shows that S-G has few layers' characteristic, consistent with the results of AFM (Figure S18, Supporting Information). XPS survey spectra of these two different types of graphene show that S-G has less oxygen content than the large-sized graphene we used before (**Figure 3**a). In addition, the quality of each graphene was also characterized. Figure 3d shows the Raman spectra of these two different types of graphene. It can be seen that S-G (graphene with low oxygen content (LO-G)) possesses extremely high quality (Figure 3b). We used the same method to disperse S-G using GO as a dispersant. After adjusting the solution to alkalinity (pH = 12), a stable and homogeneous graphene dispersion was also obtained in aqueous solution (Figure S19, Supporting Information). The zeta potential of the dispersion was found to be −47.3 mV (pH = 12) which explains the excellent stability of the dispersion (Figure S20, Supporting Information). A typical AFM image of GO/S-G hybrid was also observed (Figure S21, Supporting Information). We found that a large-sized graphene sheet can be combined with multiple GO sheets, and multiple S-G sheets can be combined with one GO sheet. These results demonstrate that whether graphene can be dispersed has no relationship with the functional groups on graphene using GO as a special "surfactant," illustrating the universality of this method.

2.3. The Mechanism of GO as a Graphene Dispersant

The effect of GO π-conjugated basal plane regions on graphene dispersion was first investigated. The π-conjugated regions on GO basal plane are closely related to the interactions with graphene. As we all know, GO dispersion is a colloidal solution.[47] Adding an electrolyte solution such as NaOH (pH = 14) into GO dispersion leads to immediate coagulation (Figure S22a,d, Supporting Information). When we mixed GO and graphene, only by stirring, or low-power ultrasound, after adding a large

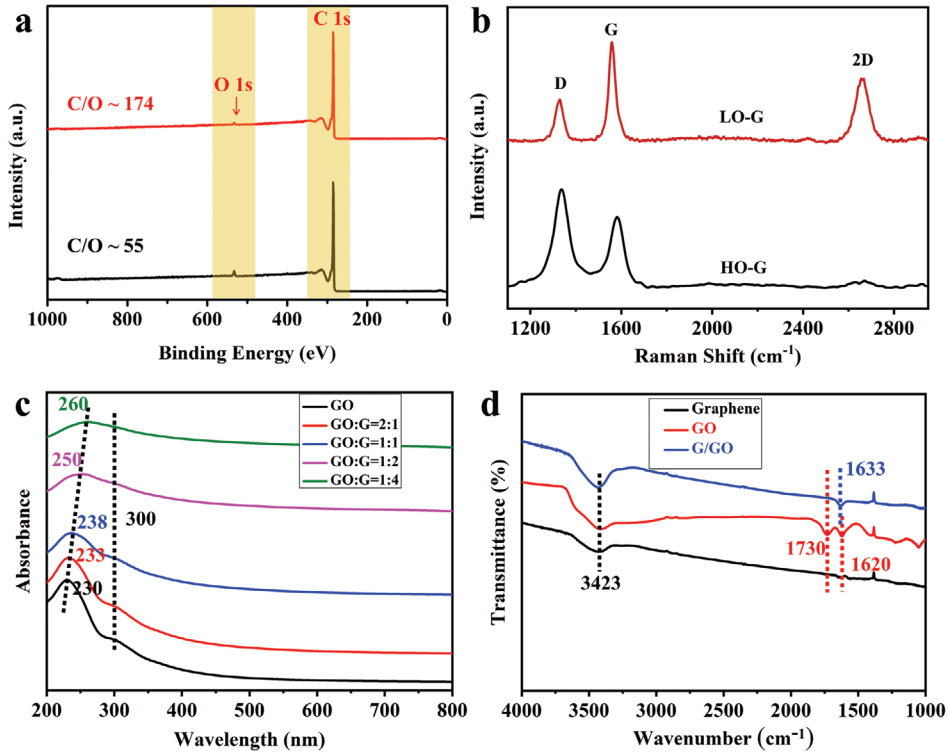

Figure 3. a) XPS survey spectra of two different types of graphene. The red curve represents small-sized graphene and the black curve represents large-sized graphene. b) Raman spectra of graphene with high oxygen content (HO-G) and graphene with low oxygen content (LO-G). c) UV–vis absorption spectra of GO and GO/G with different weight ratios (pH = 6). d) FTIR absorption spectra of GO, graphene, and GO/G (m_{GO}:m_G = 1:2, pH = 6).

amount of NaOH solution with a pH value of 14, GO sheets also precipitated rapidly, similar to Figure S22a (Supporting Information). However, because graphene sheets do not have the colloidal property, they still disperse in the aqueous solution, though the dispersion is not stable (Figure S22b,e, Supporting Information), which means that there is no interaction between GO and graphene. By contrast, when we give GO and graphene a very large force (high-power ultrasound) before adding a large amount of NaOH solution with a pH value of 14, GO and graphene complex will rapidly precipitate completely (Figure S22c,f, Supporting Information), which shows a strong combination of GO and graphene. To verify the interactions between GO and graphene, UV–visible (UV–vis) absorption spectroscopy was used to characterize dispersions with different weight ratios (m_{GO}:m_G) (Figure 3c). At 230 and 300 nm, the GO aqueous solution shows a strong absorption peak and a shoulder, corresponding to the $\pi \rightarrow \pi^*$ transition of the C=C double bond and the n $\rightarrow$ π^* transition of the C=O double bond, respectively. However, the spectrum of GO/G undergoes a redshift at 230 nm. Furthermore, as the content of graphene increases, the degree of the redshift increases, which indicates that more π-conjugated regions of GO interact with the π-conjugated domains of graphene. Besides, the Fourier-transform infrared (FTIR) spectra in Figure 3d are further verified the interaction. Compared with the C=C stretching vibrations in GO and G, the C=C stretching vibration in the GO/G is slightly shift to 1631 cm^{-1}, which is attributed mainly to π–π interactions between the GO and graphene.[48,49]

The effect of the carboxyl groups closely related to the pH values of the solution at the edge of GO on graphene dispersion was next investigated. Comparing GO sheets' size in acidic and that in alkaline solution, the size of GO sheets is much larger in acidic solution (Figure S23, Supporting Information), which is mainly attributed to the agglomeration of GO sheets. AFM images (**Figure 4**a) provide direct evidence that in acidic solution, GO sheets indeed apparently agglomerate together. The aggregate thickness of 2 nm approximates a bilayer GO stack, indicating that the aggregation of GO sheets occurs mainly at the edges (Figure 4b). In slightly acidic solution, GO sheets are homogeneously dispersed as monolayers with a thickness of ≈1 nm (Figure 4b–e). However, under alkaline solution, the size of GO sheets is similar to that in slightly acidic solution, but the average thickness of GO sheets is much higher, indicating the multilayer stacking of GO sheets (Figure 4c–f; Figure S24, Supporting Information).

Through the study of the factors affecting the amphiphilic properties of GO, the following conclusions can be drawn, as shown in Figure 4g. In the acidic solution, GO sheets can form hydrogen bonds due to the presence of a large number of carboxyl groups at their edges, causing the sheets to engage in edge-to-edge bonding.[50,51] Even if GO agglomeration occurs, a large number of π-conjugated regions that can interact with graphene are exposed on the basal plane, leading to the stable dispersion of graphene. In the alkaline solution, the edge-bound carboxylic acid groups on GO are deprotonated to carboxylates, and the hydrogen bonds are broken. As a result, the GO sheets

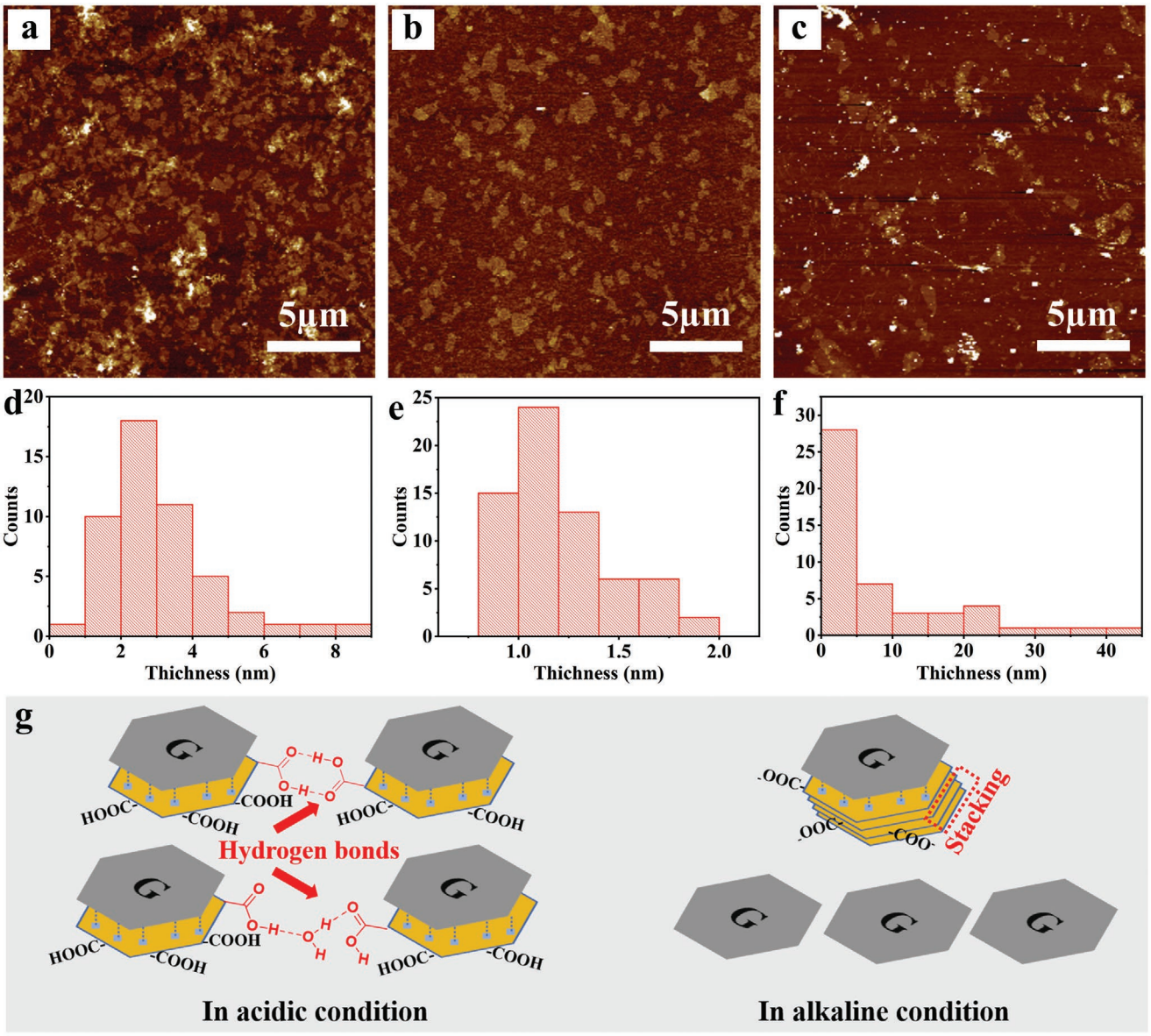

Figure 4. a–c) AFM image of GO in the acidic (pH = 2), slightly acidic (pH = 6), and alkaline (pH = 12) solutions, respectively. d–f) Size distribution of GO sheets in the acidic (pH = 2), slightly acidic (pH = 6), and alkaline (pH = 12) solutions, respectively. g) Interaction models between graphene and GO in the acidic and alkaline solutions, respectively.

tend to stack in a surface-to-surface mode to reduce their surface energy, which, in turn, blocks the π-conjugated regions on the GO basal plane. Thus, in the alkaline solution, it is difficult for GO to interact with graphene, and dispersion fails.

2.4. The Four States of GO/G

Having probed the mechanisms underlying the successful GO-directed dispersion of graphene in aqueous solution, we next explored the processability of the dispersions. Previous studies have shown that GO and carbon nanotubes' dispersions of different concentrations can be divided into four states.[29,52] In our experiment, increasing GO/G concentrations results in a continuous transition between four states, from a dilute dispersion (<10 mg mL^{-1}) to a thick paste (10–50 mg mL^{-1}), a free-standing gel (50–100 mg mL^{-1}), and eventually, a kneadable, playdough-like material (>100 mg mL^{-1}). These four states were further transformed into 1D graphene fibers, 2D graphene films, or 3D graphene doughs using various material-processing techniques (Figure S25, Supporting Information). The successful preparation of these four graphene states and three applications further highlights the excellent homogeneity and stability of GO/G.

The alignment of GO/G sheets and the compactness of the films ultimately determine electron transport behaviors in the graphene films. The preparation of highly conductive and flexible graphene films can be achieved via either simple

filtration of the dilute graphene dispersion or coating of the thick paste. The graphene films formed by filtration with alkaline GO/G display well-maintained GO/G sheets alignment and have excellent flexibility and strength, folding hundreds of times without any breaking (Figures S26 and S27, Supporting Information). In addition, **Figure 5**a shows the process of formation of a graphene film by uniformly coating GO/G thick paste on polyethylene terephthalate (PET) film. Upon drying at 45 °C, the graphene film displays well-maintained GO/G sheet alignment and can be simply removed completely. In Figure 5b, the graphene film formed simply by mixing GO/G without ultrasonic dispersion displays extremely high square resistance, while the graphene film formed from GO/G alkaline thick paste has extremely low square resistance (only 22 Ω sq^{-1}). It should be noted that after high-temperature reduction, the square resistance drops sharply, which greatly improves the conductivity. Digital images of the graphene films reveal that the films formed from simply mixed GO/G without ultrasonic

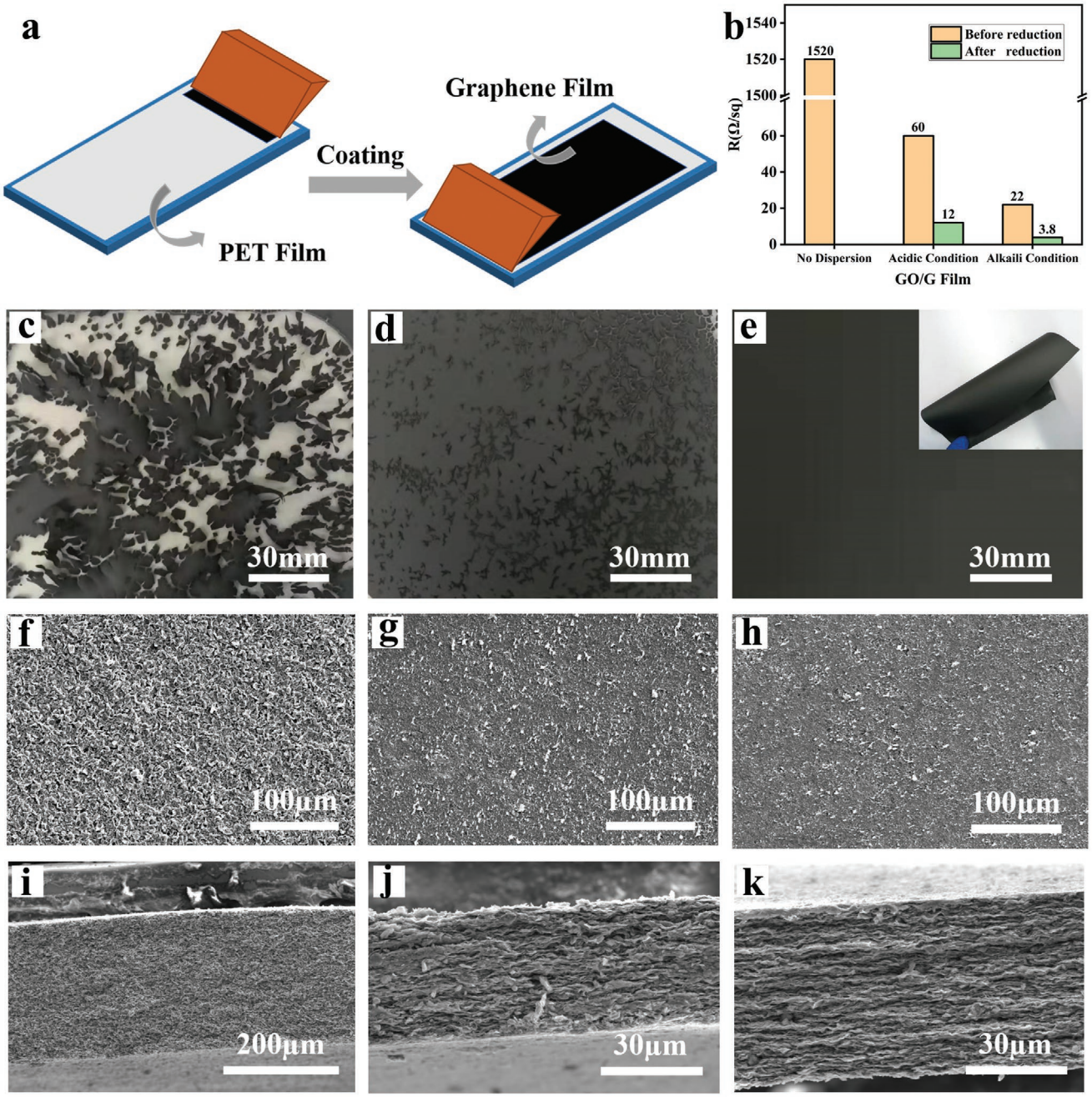

Figure 5. Highly conductive and flexible graphene films. a) Schematic diagram of coating technique for graphene films. b) Effect of dispersion methods on square resistance of coated films (m_{GO}:m_G = 1:2). c–e) Digital photographs of graphene films; the inset shows a high flexibility of graphene film prepared from alkaline GO/G. f–h) Top-view SEM images and i–k) cross-sectional SEM images of graphene film prepared from different dispersion methods.

dispersion and acidic GO/G are fragmented and inhomogeneous (Figure 5c,d), whereas the graphene film formed from the thick paste state of alkaline GO/G exhibits widespread integrity (Figure 5e). Furthermore, compared to the graphene films formed from the simply mixed GO/G and acidic GO/G (Figure 5f,g,i,j), the graphene film from alkaline GO/G displays well-maintained sheet alignment and layer-by-layer stacking, as evidenced by the planar and cross-sectional SEM images (Figure 5h,k). These data further illustrate that the alkaline graphene dispersion is more homogeneous, resulting in extremely high electrical conductivity and flexibility of related products, which maximally maintain the intrinsic properties of graphene.

In addition, graphene fibers and doughs were also prepared by different processing methods. Graphene fibers can be prepared from GO/G in thick paste state or in the more highly concentrated gel state.[52] The GO/G in the thick paste state can be wet spun into flexible graphene fibers with a diameter of 500 μm through an ethyl acetate coagulation bath by wet-spinning method (Figure S28, Supporting Information). The GO/G sheets are in an aligned orientation, resulting in graphene fibers with good flexibility, as evidenced by SEM images (Figure S29, Supporting Information). In addition, graphene fibers with millimeter-scale diameter can also be prepared through a needle tube from the more highly concentrated gel state by dry-spinning method. These fibers display excellent flexibility, which can be used to write characters directly, revealing the high stability and uniformity of the graphene dispersion in high concentration (Figure S30, Supporting Information). When the concentration of the graphene dispersion further increased, a kneadable, playdough-like material is observed. This playdough-like graphene dispersion can be formed into arbitrary shapes by common shaping methods (Figure S31, Supporting Information). In addition, after calcination at high temperature, lightweight graphene dough maintains its structural integrity without collapse, meaning that graphene sheets in the dough have a regular arrangement and strong interaction force (Figure S32, Supporting Information). These results further illustrate that GO can stably disperse graphene and form homogeneous graphene dispersions.

3. Conclusion

In summary, GO, with its abundant hydrophilic edge-bound carboxyl groups and hydrophobic π-conjugated basal plane domains, functions as a special "surfactant" to effectively disperse graphene in aqueous solution and form stable, homogeneous graphene dispersions at unprecedentedly high concentrations (>150 mg mL^{-1}). More importantly, the stability and uniformity of the graphene dispersions are determined by the pH value of GO aqueous solution and GO/G. Depending on the concentration, graphene dilute dispersions, pastes, gels, and kneadable, playdough-like material can be observed and further transformed into 1D graphene fibers, 2D graphene films, and 3D graphene doughs through various material-processing techniques. Owing to the structural similarities of GO and graphene, the prepared macroscopic graphene-based materials maximally maintain the intrinsic properties of graphene, demonstrating the immense potential of this strategy for bridging the micro- and macroscopic properties.

4. Experimental Section

All chemical reagents and solvents were commercially available without further purification. Graphene oxide dispersion and graphene powder were purchased from Changzhou Sixth Element Material Technology Co. Ltd. Other chemicals used here were purchased from Beijing Chemicals and Sino-pharm. All chemical reagents were of analytical grade. All solutions were prepared in deionized water (DI water, 18.2 MΩ cm) from a Thermo Scientific Nanopure system.

Preparation of GO-Dispersed Graphene Dispersion: The preparation method was modified from a published article.[46] In detail, GO dispersion was diluted to the proper concentration using an Ultrasonic Cell Disruption System for 1 h in an ice-water bath with 90% power (120 W) until a homogeneous solution was obtained. The graphene powder with an appropriate proportion was transferred to the above solution and was sonicated for 1 h in the ice-water bath using an Ultrasonic Cell Disruption System with 90% power (120 W). After ultrasound, the solution was adjusted to the proper alkaline using NaOH (0.1 M) to obtain homogeneous and stable graphene dispersion.

Preparation of a Continuous Transition between Four States: The preparation method was modified from a published article.[29] The preparation method of the diluted dispersion is mentioned above. The thick paste was prepared using high-pressure homogenizers. The graphene powder was transferred to the homogeneous GO dispersion and was sonicated for 10 min using high-pressure homogenizers. Then the GO/G thick paste was obtained by adjusting pH to suitable alkaline using NaOH (0.1 M). The free-standing gel and kneadable, playdough-like material were obtained by direct stirring and evaporating the GO/G thick paste.

Preparation of Graphene Films: The graphene films were prepared via either simple filtration of the dilute graphene dispersion or coating of the thick paste state. The dilute graphene dispersion was filtered using an anodic aluminum oxide filter. The resulting filter was washed with deionized water and finally dried at 45 °C overnight. The thick GO/G paste was uniformly coated using a razor blade to drag the paste to the PET film. The thickness was controlled by adjusting the screws on both ends of the rod. The coating film was left to dry at 45 °C overnight and was then torn off from the substrate to obtain graphene films.

Preparation of Graphene Fibers: The graphene fibers were prepared from GO/G in thick paste state or the highly concentrated gel state. GO/G in thick paste state was spun through an ethyl acetate coagulation bath using the wet-spinning method. After drying at 45 °C overnight, the graphene fiber was obtained. The GO/G in the concentrated gel state was loaded into a syringe and manually extruded from needles with the diameters of 1 mm, like the dry-spinning process.

Preparation of Graphene Doughs: The kneadable, playdough-like material was kneaded to the shape of a ball to make a graphene dough. A kneaded dough was sandwiched between two stainless steel foils and cold-rolled to a film with the proper thickness, which could be cut into various shapes with a razor blade or a character-shaped template. The lightweight graphene dough was prepared by calcining graphene dough at 200 °C for 15 min in an air oven.

Characterization: The morphology and detailed structure of GO and GO/G were investigated by SEM (FEI Quattro S, acceleration voltage 5–10 kV) and AFM (dimension ICON, tapping mode). Electron microscope specimens and AFM specimens were prepared by diluting GO dispersion or GO/G and added dropwise onto silicon wafers and dried at 45 °C. TEM (FEI Tecnai F30; 300 kV) and aberration-corrected atomic-resolved TEM (Titan Cubed Themis G2 300; 80 kV) were conducted to investigate the morphology and structure of graphene. Raman spectroscopy (Horiba Jobin Yvon LabRAM HR 800, 514.5 nm) and XPS (Kratos Analytical Axis-Ultra spectrometer with Al Kα X-ray source) were used to evaluate the quality, oxygen content, or impurity content of graphene and GO. Using FTIR (IRTracer-100, spectral ranges: 5000–500 cm^{-1}), specimens were prepared by freeze-drying. GO/G was immersed in a liquid nitrogen bath to freeze for 10 min. After GO dispersions were frozen, the vials were then transferred to a freeze-dryer, and porous and spongy GO foams were obtained after the ice

in frozen GO dispersions was completely sublimated. The interaction between GO and graphene was studied by UV–vis absorption spectra (Perkin Elmer Lambda 950, wavelength ranges: 200–1000 nm) and a laser particle size analyzer (Bluewave S3500). Note that the particle size measurement on this instrument is based on the assumption that the particles are spherical, so the instrument is unable to give the absolute sizes of graphene sheets. Nevertheless, the measurements obtained provide a means of monitoring dispersion stability. A four-probe resistance tester (ResMap 178) was used to test the square resistance of graphene films. A metallographic microscope (Leica Germany, DM750M) was used to observe Pickering emulsions and observe the dispersion of graphene.

Supporting Information

Supporting Information is available from the Wiley Online Library or from the author.

Acknowledgements

J.L. and L.Y. contributed equally to this work. The authors thank Yangyong Sun and Shichen Xu from Peking University and Beijing Graphene Institute for their kind suggestion and discussion on the progress of experiment. The authors thank Ying Quan from Beijing Graphene Institute for the instrument support of high-pressure homogenizer and SEM characterization of GO and GO/G. This work was supported by the Ministry of Science and Technology of China (2018YFA0703502 and 2016YFA0200104) and the National Natural Science Foundation of China (Grant Nos. 51432002, 51720105003, 21790052, 21573004, 21974004, and 51888103).

Conflict of Interest

The authors declare no conflict of interest.

Keywords

graphene dispersions, graphene oxide surfactant, pH-adjustment, tunable concentrations, ultrahigh concentrations

Received: June 3, 2020
Revised: August 31, 2020
Published online:

[1] K. S. Novoselov, V. Fal, L. Colombo, P. Gellert, M. Schwab, K. Kim, *Nature* **2012**, *490*, 192.
[2] K. S. Novoselov, A. Geim, *Nat. Mater.* **2007**, *6*, 183.
[3] V. Georgakilas, J. N. Tiwari, K. C. Kemp, J. A. Perman, A. B. Bourlinos, K. S. Kim, R. Zboril, *Chem. Rev.* **2016**, *116*, 5464.
[4] A. Ciesielski, S. Haar, M. El Gemayel, H. Yang, J. Clough, G. Melinte, M. Gobbi, E. Orgiu, M. V. Nardi, G. Ligorio, *Angew. Chem., Int. Ed.* **2014**, *53*, 10355.
[5] L. Banszerus, M. Schmitz, S. Engels, J. Dauber, M. Oellers, F. Haupt, K. Watanabe, T. Taniguchi, B. Beschoten, C. Stampfer, *Sci. Adv.* **2015**, *1*, e1500222.
[6] H. Jang, Y. J. Park, X. Chen, T. Das, M. S. Kim, J. H. Ahn, *Adv. Mater.* **2016**, *28*, 4184.
[7] G. Zhao, X. Li, M. Huang, Z. Zhen, Y. Zhong, Q. Chen, X. Zhao, Y. He, R. Hu, T. Yang, *Chem. Soc. Rev.* **2017**, *46*, 4417.
[8] G. Xin, T. Yao, H. Sun, S. M. Scott, D. Shao, G. Wang, J. Lian, *Science* **2015**, *349*, 1083.
[9] D. Parviz, S. Das, H. T. Ahmed, F. Irin, S. Bhattacharia, M. J. Green, *ACS Nano* **2012**, *6*, 8857.
[10] V. Georgakilas, M. Otyepka, A. B. Bourlinos, V. Chandra, N. Kim, K. C. Kemp, P. Hobza, R. Zboril, K. S. Kim, *Chem. Rev.* **2012**, *112*, 6156.
[11] M. Buzaglo, E. Ruse, I. Levy, R. Nadiv, G. Reuveni, M. Shtein, O. Regev, *Chem. Mater.* **2017**, *29*, 9998.
[12] A. S. Wajid, S. Das, F. Irin, H. T. Ahmed, J. L. Shelburne, D. Parviz, R. J. Fullerton, A. F. Jankowski, R. C. Hedden, M. J. Green, *Carbon* **2012**, *50*, 526.
[13] L. Zhang, Z. Zhang, C. He, L. Dai, J. Liu, L. Wang, *ACS Nano* **2014**, *8*, 6663.
[14] Y. Liang, D. Wu, X. Feng, K. Müllen, *Adv. Mater.* **2009**, *21*, 1679.
[15] X. An, T. Simmons, R. Shah, C. Wolfe, K. M. Lewis, M. Washington, S. K. Nayak, S. Talapatra, S. Kar, *Nano Lett.* **2010**, *10*, 4295.
[16] T. Sreeprasad, V. Berry, *Small* **2013**, *9*, 341.
[17] J. M. Englert, J. Röhrl, C. D. Schmidt, R. Graupner, M. Hundhausen, F. Hauke, A. Hirsch, *Adv. Mater.* **2009**, *21*, 4265.
[18] J. Cui, S. Zhou, *Chem. Mater.* **2018**, *30*, 4935.
[19] S. Sampath, A. N. Basuray, K. J. Hartlieb, T. Aytun, S. I. Stupp, J. F. Stoddart, *Adv. Mater.* **2009**, *25*, 2740.
[20] A. C. Ferrari, F. Bonaccorso, V. Fal'Ko, K. S. Novoselov, S. Roche, P. Bøggild, S. Borini, F. H. Koppens, V. Palermo, N. Pugno, *Nanoscale* **2015**, *7*, 4598.
[21] J. Park, M. Yan, *Acc. Chem. Res.* **2013**, *46*, 181.
[22] C. K. Chua, M. Pumera, *Chem. Soc. Rev.* **2013**, *42*, 3222.
[23] J. Hu, J. Hou, S. Huang, L. Zong, X. Li, Z. Zhang, Y. Duan, J. Zhang, *Carbon* **2020**, *157*, 448.
[24] L. Peng, Z. Xu, Z. Liu, Y. Guo, P. Li, C. Gao, *Adv. Mater.* **2017**, *29*, 170058.
[25] Y. Liu, P. Li, F. Wang, W. Fang, Z. Xu, W. Gao, C. Gao, *Carbon* **2019**, *155*, 462.
[26] D. A. Dikin, S. Stankovich, E. Zimney, R. D. Piner, G. Dommett, G. Evmenenko, S. T. Nguyen, R. S. Ruoff, *Nature* **2017**, *448*, 457.
[27] Z. Xu, Y. Zhang, P. Li, C. Gao, *ACS Nano* **2012**, *6*, 7103.
[28] B. Fang, D. Chang, Z. Xu, C. Gao, *Adv. Mater.* **2020**, *32*, 1902664.
[29] C. N. Yeh, H. Huang, A. T. O. Lim, R. H. Jhang, C. H. Chen, J. Huang, *Nat. Commun.* **2019**, *10*, 422.
[30] D. Myers, *Surfactant Science and Technology*, John Wiley & Sons, Hoboken, NJ **2005**.
[31] K. Zang, X. Zhang, H. Li, X. Xing, L. E. Jin, Q. Cao, P. Li, *J. Mater. Sci.* **2018**, *53*, 2484.
[32] A. Lerf, H. He, M. Forster, J. Klinowski, *J. Phys. Chem. B* **1998**, *102*, 4477.
[33] D. Li, M. B. Müller, S. Gilje, R. B. Kaner, G. G. Wallace, *Nat. Nanotechnol.* **2008**, *3*, 101.
[34] D. Li, R. B. Kaner, *Science* **2008**, *320*, 1170.
[35] S. Park, R. S. Ruoff, *Nat. Nanotechnol.* **2009**, *4*, 217.
[36] L. J. Cote, J. Kim, V. C. Tung, J. Luo, F. Kim, J. Huang, *Pure Appl. Chem.* **2010**, *83*, 95.
[37] J. Kim, L. J. Cote, J. Huang, *Acc. Chem. Res.* **2012**, *45*, 1356.
[38] S. N. Kazi, A. Badarudin, M. Zubir, H. Ming, M. Misran, E. Sadeghinezhad, M. Mehrali, N. Syuhada, *Nanoscale Res. Lett.* **2015**, *10*, 212.
[39] M. Zubir, A. Badarudin, S. N. Kazi, H. Ming, R. Sadri, A. Amiri, *J. Dispersion Sci. Technol.* **2015**, *37*, 1395.
[40] S. Stankovich, D. A. Dikin, R. D. Piner, K. A. Kohlhaas, A. Kleinhammes, Y. Jia, Y. Wu, S. T. Nguyen, R. S. Ruoff, *Carbon* **2007**, *45*, 1558.
[41] D. Yang, A. Velamakanni, G. Bozoklu, S. Park, M. Stoller, R. D. Piner, S. Stankovich, I. Jung, D. A. Field, C. A. Ventrice Jr., *Carbon* **2009**, *47*, 145.
[42] K. Krishnamoorthy, M. Veerapandian, K. Yun, S. J. Kim, *Carbon* **2013**, *53*, 38.

[43] A. Kovtun, D. Jones, S. Dellelce, E. Treossi, A. Liscio, V. Palermo, *Carbon* **2019**, *143*, 268.
[44] K. Erickson, R. Erni, Z. Lee, N. Alem, W. Gannett, A. Zettl, *Adv. Mater.* **2010**, *22*, 4467.
[45] L. Tian, M. J. Meziani, F. Lu, C. Y. Kong, L. Cao, T. J. Thorne, Y. P. Sun, *ACS Appl. Mater. Interfaces* **2010**, *2*, 3217.
[46] J. Kim, L. J. Cote, F. Kim, W. Yuan, K. R. Shull, J. Huang, *J. Am. Chem. Soc.* **2010**, *132*, 8180.
[47] D. Li, M. B. Muller, S. Gilje, R. B. Kaner, G. G. Wallace, *Nat. Nanotechnol.* **2008**, *3*, 101.
[48] H. D. Huang, S. Y. Zhou, P. G. Ren, X. Ji, Z.-M. Li, *RSC Adv.* **2015**, *5*, 8073.
[49] R. Algaashani, A. Najjar, Y. Zakaria, S. Mansour, M. A. Atieh, *Ceram. Int.* **2019**, *45*, 14439.
[50] C. Valtierrez-Gaytan, I. Ismail, C. Macosko, B. L. Stottrup, *Colloids Surf., A* **2017**, *529*, 434.
[51] R. A. Soler-Crespo, W. Gao, L. Mao, H. T. Nguyen, M. R. Roenbeck, J. T. Paci, J. Huang, S. T. Nguyen, H. D. Espinosa, *ACS Nano* **2018**, *12*, 6089.
[52] K. Chiou, S. Byun, J. Kim, J. Huang, *Proc. Natl. Acad. Sci. USA* **2018**, *115*, 5703.